nature geoscience

ARTICLES

https://doi.org/10.1038/s41561-019-0512-6

A thick crustal block revealed by reconstructions of early Mars highlands

Sylvain Bouley[1,2*], James Tuttle Keane[3], David Baratoux[4], Benoit Langlais[5], Isamu Matsuyama[6], Francois Costard[1], Roger Hewins[7], Valerie Payré[8], Violaine Sautter[7], Antoine Séjourné[1], Olivier Vanderhaeghe[4] and Brigitte Zanda[2,7]

The global-scale crustal structure of Mars is shaped by impact basins, volcanic provinces, and a hemispheric dichotomy with a thin crust beneath the northern lowlands and a thick crust beneath the southern highlands. The southern highlands are commonly treated as a coherent terrain of ancient crust with a common origin and shared geologic history, plausibly originating from a giant impact(s) or a hemispheric-scale mantle upwelling. Previous studies have quantified the contribution of volcanism to this crustal structure; however, the influence of large impacts remains unclear. Here we present reconstructions of the past crustal thickness of Mars (about 4.2 Gyr ago) where the four largest impact basins (Hellas, Argyre, Isidis and Utopia) are removed, assuming mass conservation, as well as the main volcanic provinces of Tharsis and Elysium. Our reconstruction shows more subdued crustal thickness variations than at present, although the crustal dichotomy persists. However, our reconstruction reveals a region of discontinuous patches of thick crust in the southern highlands associated with magnetic and geochemical anomalies. This region, corresponding to Terra Cimmeria–Sirenum, is interpreted as a discrete crustal block. Our findings suggest that the southern highlands are composed of several crustal blocks with different geological histories. Such a complex architecture of the southern highlands is not explained by existing scenarios for crustal formation and evolution.

The crust of Mars has been shaped by 4.5 Gyr of meteorite impacts, volcanism, tectonism and surface processes (Fig. 1a,b). Its most prominent crustal features are the hemispheric dichotomy, the Tharsis volcanic province and several large impact basins. The hemispheric dichotomy describes Mars's north–south asymmetry, where the northern lowlands have roughly half the crustal thickness of the southern highlands. The Tharsis volcanic province represents the thickest region of the crust and is associated with a prominent topographic rise responsible for deformation of the lithosphere at a planetary scale[1]. Whereas the crustal thickness of Tharsis is considered to be the result of magmatic intrusions and volcanic eruptions, the origin of the hemispheric dichotomy is more enigmatic. Past studies have suggested that the hemispheric crustal dichotomy is the result of either giant impact(s)[2,3] or hemispheric-scale mantle upwelling[4,5].

While previous studies have quantified the contribution of Tharsis to Mars's gravity field[1], crustal thickness[6] and topography[7], the contribution of impact basins to the crustal structure has never been quantified. Mars has four giant (diameters >1,000 km) unequivocal impact basins with unambiguous gravity field anomalies and expressions in crustal thickness maps (Hellas, Argyre, Utopia and Isidis), but only three of them have a significant topographic expression (Hellas, Argyre and Isidis). Utopia has a muted topographic signature, due to its early formation and possible crustal relaxation[8]. The four impacts (Hellas, Argyre, Isidis and Utopia) predate Tharsis, and extensively modified Mars's crustal structure. For example, Hellas is surrounded by an annulus of high-standing topography and thickened crust, which has been interpreted to be the consequence of ejecta deposits and crustal thickening during crater excavation and collapse[9–11] (Extended Data Fig. 1). Several outcrops in Terra Cimmeria and Terra Sirenum are interpreted as a veneer of Hellas ejecta over older crust—roughly four crater radii away from the centre of the basin[12]. Investigations of lunar gravity and topography, coupled with hydrocode impact simulations, have suggested that the Moon's hemispheric dichotomy (where the far-side crust is about twice as thick as the nearside crust) may be partially explained by the deposition of a thick ejecta blanket around the giant South Pole–Aitken impact basin[13,14]. Extrapolating these results to Mars, it appears necessary to determine the contribution of large impact basins to its present crustal structure.

Reconstructing Mars without impact basins and volcanoes

There are many methods for isolating, characterizing and removing the contribution of impact basins and volcanoes from the gravity field and topography of planets—each with varying degrees of complexity[1,6,15,16]. In this work we develop a method for removing these features using crustal thickness maps[17,18] (Fig. 1c,d). These maps—which are derived from topography and gravity data (Methods)—can be used for reconstruction of the early crustal structure with conservation of mass arguments. The present crustal thickness model (model B, ref. [18]) accounts for higher crustal densities in volcanic complexes (2,900 kg m^{-3}), lower crustal densities elsewhere (2,582 kg m^{-3}) and a mantle density of 3,500 kg m^{-3}. To simplify calculations, the crustal thickness was rescaled at every location to the same crustal density (that is, we increase (decrease) the crustal

[1]GEOPS – Géosciences Paris Sud, Univ. Paris-Sud, CNRS, Université Paris-Saclay, Orsay, France. [2]IMCCE – Observatoire de Paris, CNRS-UMR 8028, Paris, France. [3]California Institute of Technology, Pasadena, CA, USA. [4]Geosciences Environnement Toulouse, UMR 5563 CNRS, IRD & Université de Toulouse, Toulouse, France. [5]Laboratoire de Planétologie et Géodynamique, CNRS UMR 6112, Université de Nantes, Université d'Angers, Nantes, France. [6]Lunar and Planetary Laboratory, University of Arizona, Tucson, AZ, USA. [7]Institut de Minéralogie, de Physique des Matériaux, et de Cosmochimie (IMPMC) – Sorbonne Université- Muséum National d'Histoire Naturelle, UPMC Université Paris 06, UMR CNRS 7590, IRD UMR 206, Paris, France. [8]Department of Earth, Environmental and Planetary Sciences, Rice University, Houston, TX, USA. *e-mail: sylvain.bouley@u-psud.fr

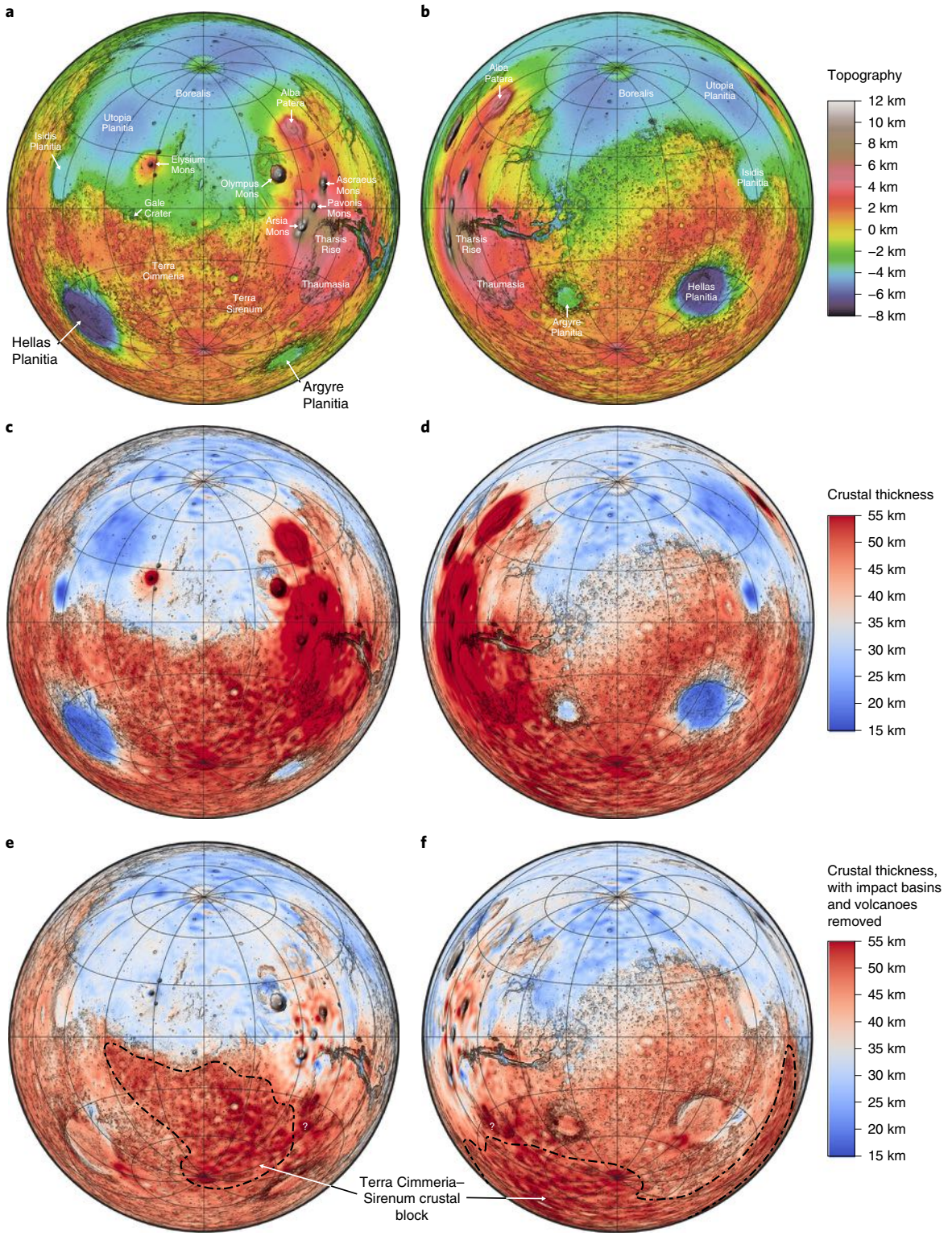

Fig. 1 | A global view of the crustal structure of Mars. a,**b**, The Mars Orbiter Laser Altimeter topography of Mars with the features of interest labelled[9]. **c**,**d**, The crustal thickness of Mars based on crustal model B (ref. [18], Methods). **e**,**f**, The crustal thickness of Mars after removing all of the large impact basins and volcanic features. The Cimmeria–Sirenum crustal block is enclosed by a dash–dot line. The question mark to the east of the block indicates the unclear boundary between the Thaumasia region and the Cimmeria–Sirenum block due to the possible specific origin of Thaumasia[19]. The maps are in Lambert azimuthal equal-area projection, centred on the equator at longitudes 0° (left column) and 180° (right column). Each map covers all of Mars except for a small region antipodal to the map centre. The maps are overlaid on the present-day topography for reference. Grid lines are in increments of 30° of latitude and longitude.

thickness in regions of high (low) density until the crustal density is globally uniform). This lets us use crustal mass and crustal volume conservation interchangeably.

We assume that impacts and volcanoes modify the crustal structure symmetrically about their centres, and that impact basins reshape the crust in a manner that approximately conserves crustal

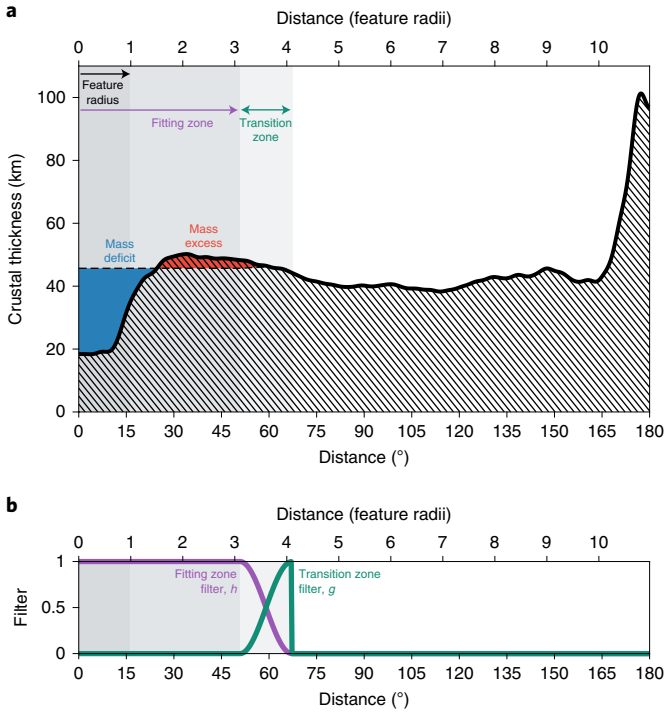

Fig. 2 | The radial crustal structure of Hellas Planitia. a, The azimuthally average crustal thickness about Hellas (solid black line with hatching beneath). We calculate the mean crustal thickness in the transition zone, and then calculate the mass of crustal material above and below that datum within the 'fitting zone'. The mass above the mass-conserving crustal thickness (the mass excess, red) integrated in an annulus around the feature is equal to the mass below it (the mass deficit, blue). The peak at 180° distance is Alba Patera, which is approximately antipodal to Hellas. **b**, The fitting and transition zone filters used in this reconstruction (Methods).

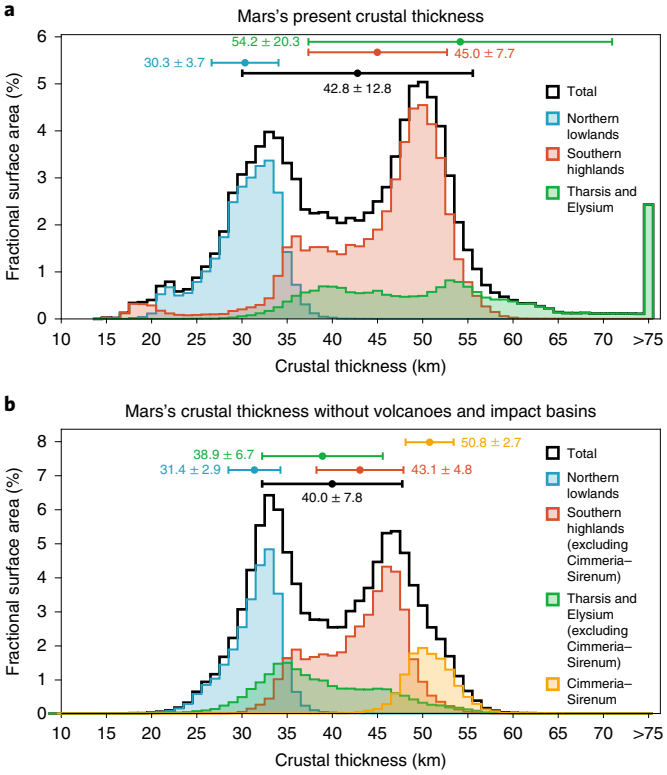

Fig. 3 | Histograms of crustal thickness of three domains (northern lowlands, southern highlands and Cimmeria–Sirenum) of the Martian crust. a, Mars's present crustal thickness. **b**, Mars's crustal thickness without volcanoes and impact basins. Note that the contribution of Tharsis and Elysium is isolated to the northern lowlands to visualize the residual contribution after removal. The black histograms show the global distribution of crustal thickness; when summed together, those coloured histograms equal the global histogram. The horizontal error bars indicate the mean and standard deviation for each respective distribution.

mass. Figure 2 shows an example of our fitting process for the Hellas basin. To remove the feature of interest, we first calculate the azimuthally averaged crustal thickness as a function of distance from the centre of the feature (Fig. 2a). Next, we define an annulus outside the feature (the 'transition zone', Fig. 2a,b), which we take to represent the background crustal thickness. We calculate the mean crustal thickness in the transition zone, and then calculate the mass of crustal material above and below that datum within the 'fitting zone'. If the mass above the datum (the mass excess) equals the mass below the datum (the mass deficit), then we deem the background crustal thickness to be a mass-conserving solution. We include a cosine taper to prevent discontinuities in the corrected crustal thickness map. For each feature of interest, we performed a parameter-space search for mass-conserving crustal structure corrections—testing a range of possible transition zone radii and widths (Extended Data Fig. 3). In cases where multiple mass-conserving solutions are found, we select the solution that makes the smallest change to the crustal structure. In cases where no mass-conserving solution is found, we select the solution that comes closest to conserving mass. While the formation of impact basins should conserve crustal mass, the same cannot be assumed for large volcanic edifices (as the erupted mass may be derived from the mantle and not the crust). Thus, for removing volcanoes, we prescribe a nominal angular radius of the feature based on the slope break at its edge that is identified on the azimuthally averaged crustal thickness profiles. We then remove the crustal mass above the background, defined from an average value in an annulus surrounding the volcanic province (Extended Data Fig. 4).

Using this technique, we sequentially isolated and removed the axisymmetric crustal thickness structures associated with the four largest impact basins (Hellas (Fig. 2), Argyre, Isidis and Utopia), Elysium Mons and the Tharsis Rise, plus the five largest individual volcanoes: Olympus Mons, Arsia Mons, Pavonis Mons, Ascraeus Mons and Alba Patera. This method is iterative and nonlinear. That is, starting with the present crustal thickness of Mars, we remove one feature, and then use that iterated crustal thickness as the starting point for removing the next feature, and so on (Extended Data Fig. 5). This means that the resulting corrected crustal structure depends a priori on the order in which we remove features, although the effect of the order is minimal if the features are distant enough from each other, which is the case here. To evaluate this dependence, we repeated this analysis using randomized removal sequences. We find that the solution is only weakly dependent on the order of removal (Methods). With this precaution taken, our nominal solution uses a removal sequence based on our current knowledge of the relative chronology of basins and volcanoes[8], from youngest to oldest: Elysium, Olympus and Tharsis montes, Tharsis Rise, Argyre, Isidis, Hellas and Utopia.

Subdued thickness variations of the early Martian crust

Removing impact basins and volcanic constructs reveals more subdued crustal thickness variations (Figs. 1e,f and 3). The hemispheric dichotomy persists in the reconstruction. Hellas contributes to the southern highlands, but excavation of the basin and emplacement

of ejecta are unable to explain the entire dichotomy; the mass excess in the southern highlands is about four times larger than the mass deficit within the Hellas basin.

However, after removing all of the large impact basins and volcanic features, the crustal thickness map highlights a crustal block characterized by discontinuous, thick (>50 km) regions corresponding to Terra Cimmeria–Sirenum (Fig. 1e,f). We delineated the boundary of this block such that it includes all of the neighbouring >50-km-thick crustal segments (Extended Fig. 6). We excluded the Thaumasia region, even though it has comparable thickness, because it may have a different tectonic (orogenic) history[19]. The relation between the most eastern part of the Terra Cimmeria–Sirenum crustal block and Thaumasia is unclear (Fig. 1e,f).

The distribution of crustal thicknesses suggests that the early Martian crust can be divided into three main crustal domains having characteristic thickness ranges that partially overlap (Fig. 3b): the northern lowlands with a thickness of between 20 and 38 km (centred at 33 km); the southern highlands—including Arabia Terra, Hellas and Argyre—with an intermediate thickness of between 30 and 55 km (centred at 46 km); and the Terra Cimmeria–Sirenum block with a thickness of between 42 and 60 km (centred at 50 km).

A thick crustal block in the southern highlands

The Cimmeria–Sirenum crustal block is also noticeable because it shares many of the characteristics of terrestrial continental crust. On Earth, continental crust is derived via differentiation and remelting of pre-existing basaltic crust. It possesses an intermediate composition between felsic and mafic, is enriched in incompatible elements, and is associated with thicker crust and elevated topography. The Terra Cimmeria–Sirenum region is associated with anomalously elevated pre-Tharsis topography[20] (Extended Data Fig. 7) and includes the strongest crustal magnetic anomalies[21–24] (Fig. 4a), which, by comparison with the Earth, could correspond to the accretion of terranes[25]. Terra Cimmeria–Sirenum is also associated with some of the highest surface (down to the first metre) abundances of potassium (K) and thorium (Th) (Fig. 4b,c)[26]. This region is the only place in the southern terrains where K and Th are correlated. Within this region, lower concentrations of K and Th are noted in the region near the south pole, where ground ice may mask the true (ice-free) K and Th (ref. [26]). Only the most eastern part of the crustal block (~10% of its surface area) is not associated with these geochemical and magnetic anomalies. Possible fragments of continental crust have been found with in situ observations by the Curiosity rover at Gale crater[27] on the northern edge of the Cimmeria–Sirenum block (Fig. 1a). While this interpretation appears inconsistent with the vast amount of spectroscopic observations suggesting that the surface of this region is dominated by basaltic rock[28], it is plausible that these basalts are surficial deposits overlying a geochemically distinct crust. This would explain why exposed continental components are rare in the southern hemisphere[29].

The existence of (at least) one crustal block on Mars makes the pre-Noachian geologic history of Mars—and the origin of the hemispheric dichotomy—much more complex than previously recognized. We identify a regional-scale crustal block covering 10% of Mars. Geophysical and geochemical signatures in this region are suggestive of a geochemically evolved crustal component. Combined with the identification of continental crust-like material on Mars in specific outcrops[30], and inferred from meteoritic samples containing zircons[27,31,32], our findings suggest that the Cimmeria–Sirenum crustal block had a complex geologic history, whether or

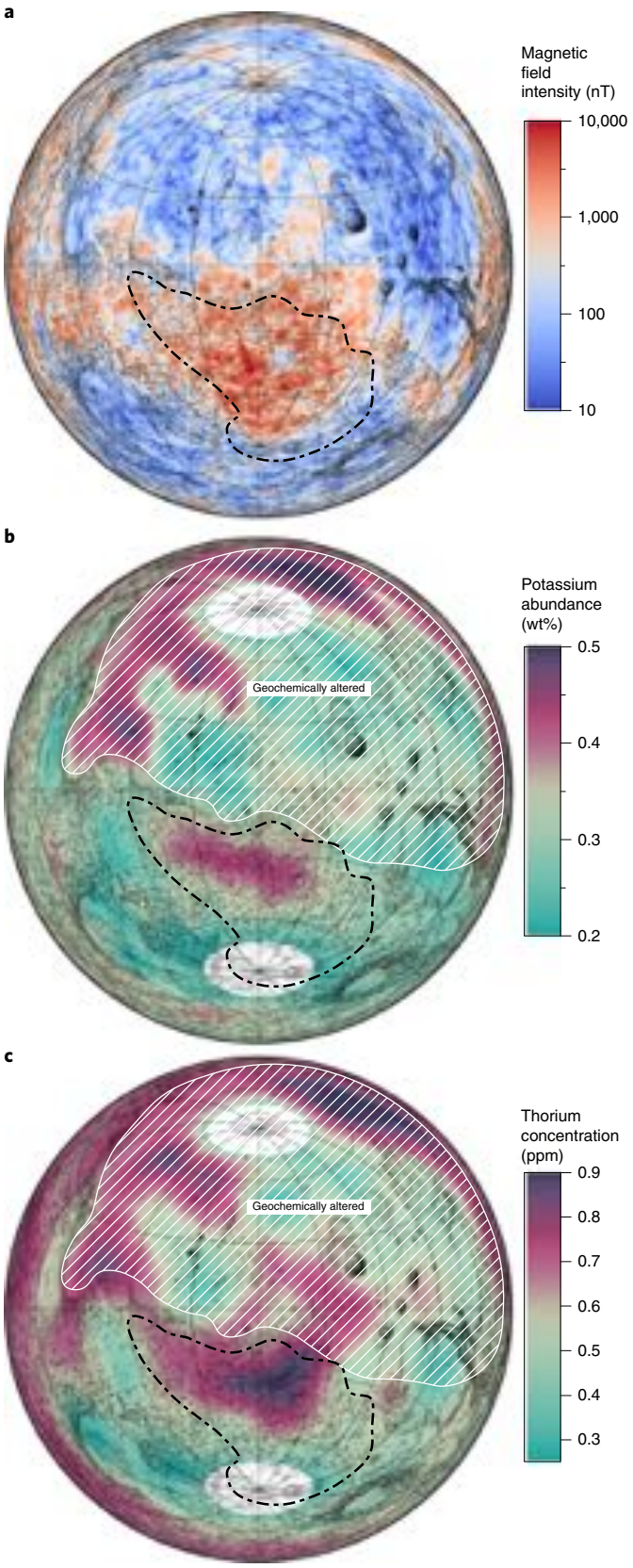

Fig. 4 | The geophysical and geochemical signature of the Cimmeria–Sirenum block. a, The magnetic field intensity, evaluated at the surface of Mars[24]. **b**, The potassium concentration (wt%)[26]. **c**, The thorium concentration (ppm)[26]. In **b** and **c**, the northern hemisphere is hatched out to focus attention on the signatures south of the dichotomy. The maps are in Lambert azimuthal equal-area projection, centred on 0°, and cover all of Mars except for a small region on the opposite hemisphere. The maps are overlaid on the present-day topography for reference. The Cimmeria–Sirenum crustal block is enclosed by a dash-dot line.

not it is analogous to terrestrial continental crust. Since this terrain is overprinted by the Hellas and Argyre basins, it is probably the oldest part of the crust. Subsequent large impacts significantly altered Mars's crustal structure and contributed to the observed hemispheric dichotomy. Therefore, the southern highlands should not be considered as a single, homogeneous unit (requiring a single formation mechanism), but rather a collection of crustal blocks with plausibly different origins, variably affected by magmatic, tectonic and impact processes. The formation mechanism of several crustal blocks during the pre-Noachian (before 4.1 Gyr ago) remains to be deciphered and has important implications for the planet's evolution, including its climate, the surface environment and the mantle dynamics.

Online content

Any methods, additional references, Nature Research reporting summaries, source data, extended data, supplementary information, acknowledgements, peer review information; details of author contributions and competing interests; and statements of data and code availability are available at https://doi.org/10.1038/s41561-019-0512-6.

Received: 26 January 2019; Accepted: 19 November 2019;
Published online: 06 January 2020

References

1. Zuber, M. T. & Smith, D. E. Mars without Tharsis. *J. Geophys. Res.* **102**, 28673–28686 (1997).
2. Wilhelms, D. E. & Squyres, S. W. The martian hemispheric dichotomy may be due to a giant impact. *Nature* **309**, 138–140 (1984).
3. Frey, H. & Shultz, R. A. Large impact basins and the mega-impact origin for the crustal dichotomy on Mars. *Geophys. Res. Lett.* **15**, 229–232 (1988).
4. Zhong, S. & Zuber, M. T. Degree-1 mantle convection and the crustal dichotomy on Mars. *Earth Planet. Sci. Lett.* **189**, 75–84 (2001).
5. Roberts, J. H. & Zhong, S. Degree-1 convection in the Martian mantle and the origin of the hemispheric dichotomy. *J. Geophys. Res.* **111**, E06013 (2006).
6. Andrews-Hanna, J. C., Zuber, M. T. & Banerdt, W. B. The Borealis basin and the origin of the martian crustal dichotomy. *Nature* **453**, 1212–1215 (2008).
7. Matsuyama, I. & Manga, M. Mars without the equilibrium rotational figure, Tharsis, and the remnant rotational figure. *J. Geophys. Res. Planets* **115**, 12020 (2010).
8. Fassett, C. I. & Head, J. W. Sequence and timing of conditions on early Mars. *Icarus* **211**, 1204–1214 (2011).
9. Smith, D. E. et al. The global topography of Mars and implications for surface evolution. *Science* **284**, 1495–1503 (1999).
10. Zuber, M. T. et al. Internal structure and early thermal evolution of Mars from Mars Global Surveyor topography and gravity. *Science* **287**, 1788–1793 (2000).
11. Zuber, M. The crust and mantle of mars. *Nature* **412**, 220–227 (2001).
12. Irwin, R. P., Tanaka, K. L. & Robbins, S. J. Distribution of Early, Middle, and Late Noachian cratered surfaces in the Martian highlands: implications for resurfacing events and processes. *J. Geophys. Res. Planets* **118**, 278–291 (2013).
13. Melosh, H. J. et al. South Pole–Aitken basin ejecta reveal the Moon's upper mantle. *Geology* **45**, 1063–1066 (2017).
14. Zuber, M. T., Smith, D. E., Lemoine, F. G. & Neumann, G. A. The shape and internal structure of the Moon from the clementine mission. *Science* **266**, 1839–1843 (1994).
15. Keane, J. T. & Matsuyama, I. Evidence for lunar true polar wander and a past low-eccentricity, synchronous lunar orbit. *Geophys. Res. Lett.* **41**, 6610–6619 (2014).
16. Garrick-Bethell, I., Perera, V., Nimmo, F. & Zuber, M. T. The tidal-rotational shape of the Moon and evidence for polar wander. *Nature* **512**, 181–184 (2014).
17. Genova, A. et al. Seasonal and static gravity field of Mars from MGS, Mars Odyssey and MRO radio science. *Icarus* **272**, 228–245 (2016).
18. Goossens, S. et al. Evidence for a low bulk crustal density for Mars from gravity and topography. *Geophys. Res. Lett.* **44**, 7686–7694 (2017).
19. Nahm, A. L. & Schultz, R. A. Evaluation of the orogenic belt hypothesis for the formation of the Thaumasia highlands, Mars. *J. Geophys. Res.* **115**, E04008 (2010).
20. Bouley, S. et al. Late Tharsis formation and implications for early Mars. *Nature* **531**, 344–347 (2016).
21. Connerney, J. E. P. et al. The global magnetic field of Mars and implications for crustal evolution. *Geophys. Res. Lett.* **28**, 4015–4018 (2001).
22. Arkami-Hamed, J. A coherent model of the crustal magnetic field of Mars. *J. Geophys. Res.* **109**, E09005 (2004).
23. Langlais, B., Purucher, M. E. & Mandea, M. Crustal magnetic field of Mars. *J. Geophys. Res.* **109**, E02008 (2004).
24. Langlais, B. et al. A new model of the crustal magnetic field of Mars using MGS and MAVEN. *J. Geophys. Res. Planets* **124**, 1542–1569 (2019).
25. Fairén, A. G., Ruiz, J. & Anguita, F. An origin for the linear magnetic anomalies on Mars through accretion of terranes: implications for dynamo timing. *Icarus* **160**, 220–223 (2002).
26. Boynton, W. V. et al. Concentration of H, Si, Cl, K, Fe, and Th in the low- and mid-latitude regions of Mars. *J. Geophys. Res.* **112**, E12S99 (2007).
27. Sautter, V. et al. In situ evidence for continental crust on early Mars. *Nat. Geosci.* **8**, 605–609 (2015).
28. Rogers, A. D. et al. Global spectral classification of Martian low-albedo regions with Mars Global Surveyor Thermal Emission Spectrometer (MGS-TES) data. *J. Geophys. Res.* **112**, E02004 (2007).
29. Baratoux, D. et al. Petrological constraints on the density of the Martian crust. *J. Geophys. Res. Planets* **119**, 1707–1727 (2014).
30. Christensen, P. R. et al. Evidence for magmatic evolution and diversity on Mars from infrared observations. *Nature* **436**, 504–509 (2005).
31. Humayun, M. et al. Origin and age of the earliest Martian crust from meteorite NWA 7533. *Nature* **503**, 513–516 (2013).
32. Bouvier, L. C. et al. Evidence for extremely rapid magma ocean crystallization. *Nature* **586**, 586–589 (2018).

Methods

Crustal thickness models. The combination of gravity and topography provides a unique insight into the interior structure of planetary bodies—including their crustal thickness[33]. Unfortunately, models of crustal thickness are inherently non-unique due to the degeneracy involved in inverting planetary gravity fields. Crustal thickness models require assumptions about the spectral characteristics of the crust/mantle interface, density of the crust and mantle (including lateral and vertical variations thereof), minimum crustal thickness and so on. To mitigate some of these degeneracies, we consider two different, published crustal thickness models: model A (ref. [17]) assumes a globally constant crustal density (2,900 kg m^{-3}) and model B (ref. [18]) assumes a higher crustal density in volcanic complexes (2,900 kg m^{-3}) and a lower crustal density elsewhere (2,582 kg m^{-3}). Goossens et al.[18] also considered a model with laterally varying crustal density constrained by short-wavelength gravity data (model C), although we did not use this model because these crustal densities are poorly constrained—particularly in the southern hemisphere and Cimmeria–Sirenum in particular. For both models we arrive at the same conclusion: the Cimmeria–Sirenum region is anomalously thick. Throughout this manuscript, we use model B, unless stated otherwise.

Removing the contribution of impact basins with conservation of mass. We assume that impact basins reshaped the crustal structure of Mars in a way that approximately conserved crustal mass. Here we describe the method by which we reconstruct Mars's early crustal structure using conservation of mass.

The first step in this process is translating crustal thickness maps into data products that more directly enable us to test mass conservation. For model A, the crustal density is the same everywhere, meaning that we can consider mass conservation by merely conserving crustal volume (that is, crustal thickness × surface area). However, the same is not true for model B, because this model has a spatially varying crustal density. We accommodate this by rescaling the crustal thickness to the same crustal density (2,582 kg m^{-3}) everywhere. This scaling preserves crustal mass, and slightly increases the crustal thickness in regions with a higher crustal density (that is, volcanoes). Since we do not force mass conservation in volcanoes, this has a negligible effect on the crustal reconstruction. We detail this here only for completeness.

For each feature of interest, we calculate the azimuthally averaged crustal thickness profile, $H(\gamma)$, as a function of the radial distance from the centre of the feature, γ. This is achieved by interpolating the gridded crustal thickness models at a distance from the centre of the feature, γ, for all azimuths (0°–360°) and taking the mean (for example, Extended Data Figs. 1 and 2).

Determining whether a crustal thickness profile conserves mass requires assumptions about the size of the region over which we expect mass to be conserved, and the background (pre-impact) crustal thickness. To avoid making arbitrary choices, we perform a parameter-space search for each feature of interest to determine the best mass-conserving structure. For each feature, we construct two related filters: one describing the 'fitting zone' where we expect mass to be conserved, and one describing an annulus around the fitting zone that we expect to represent the background crustal thickness (the 'transition zone'; Fig. 2). The fitting zone filter, $f(\gamma)$, is defined as 1 within the fitting zone ($\gamma \leq a$), tapering by a cosine taper to 0 by the outer edge of the transition zone ($\gamma = b$). The transition zone filter, $g(\gamma)$, is defined as 0 within the fitting zone ($\gamma \leq a$), tapering by a cosine taper to 1 by the outer edge of the transition zone ($\gamma = b$), and then defined as 0 beyond the transition zone ($\gamma > b$). In the transition zone, $g(\gamma) = 1 - f(\gamma)$. The use of a cosine taper results in a smoother fit and prevents sharp discontinuities in the resulting corrected crustal thickness maps.

We calculate the background crustal thickness, H_0, by taking the mean of the crustal thickness in the transition zone, weighted by the transition zone filter, $g(\gamma)$, and the surface area in that annulus, $S(\gamma)$:

$$H_0 = \frac{\Sigma H(\gamma) S(\gamma) g(\gamma)}{\Sigma S(\gamma) g(\gamma)}$$

where $S(\gamma)$ is defined as:

$$S(\gamma) = 2\pi R^2 [\cos(\gamma - \delta\gamma) - \cos(\gamma + \delta\gamma)]$$

and R is the radius of Mars (3,396 km), and $\delta\gamma$ is one-half of the step-size between successive radial distances, γ.

Next, we can apply the background crustal thickness, H_0, to the fitting zone and determine whether mass is conserved within that region. We calculate the mass anomaly, $M(\gamma)$:

$$M(\gamma) = S(\gamma)[H(\gamma) f(\gamma) - H_0 f(\gamma)]$$

where $M(\gamma)$ is positive if the crustal thickness in a given annulus is above H_0, and $M(\gamma)$ is negative if the crustal thickness in a given annulus is below H_0. By summing all positive mass anomalies, we can calculate the total mass excess, $M^+ = \Sigma M$ (if $M > 0$), and we similarly calculate the total mass deficit by summing all negative mass anomalies, $M^- = \Sigma M$ (if $M < 0$). Mass is conserved if $M^+ = |M^-|$. We define the mass balance as the ratio of mass excess to mass deficit, $B = |M^+/M^-|$. If $B = 1$, then mass is conserved.

We repeat the process above for a range of possible fitting zone and transition zone sizes, and calculate the mass balance for each case. Extended Data Fig. 3 shows an example output of this parameter-space search. Mass-conserving solutions are identified by having mass balances equal to 1. For most features, there are multiple mass-conserving solutions—often highlighting correlations between the fitting parameters. In such cases, it is necessary to further constrain the mass-conserving solutions, and ultimately pick a single solution to implement. To do this, we select the mass-conserving solution with the smallest fitting zone size, between 1 and 5× the feature radius, and the smallest transition zone radius, greater than 1× the feature radius. The feature radius is the radius of the impact basin in question. This criterion is aimed at requiring the smallest structural change, and partly motivated by analytic models and empirical data that suggest that impact basins tend to deposit most of their ejecta within one crater diameter of the basin rim[34]. In practice, the solutions are not strongly sensitive to these constraints, and the mass-conserving solutions tend to be indistinguishable (for example, Extended Data Fig. 3b,d). In some cases, no reasonable mass-conserving solutions can be found. In these instances, we follow the same bounding constraints listed above and select the solution that comes the closest to conserving mass (that is, the solution that minimizes the quantity $M^+ - |M^-|$). While it is not immediately obvious that this method would be appropriate for scenarios where mass may not be conserved, we find that this approach tends to result in crustal thickness corrections close to what we would pick if we had selected the fitting zone and background crustal thickness by hand (as we do with volcanoes).

While more complicated crustal-correction methods exist[1,6,15,16], our mass-conservation approach yields the same qualitative results as many past approaches. Furthermore, while it was not noted as unusual, the Cimmeria–Sirenum crustal block stands out in previous crustal correction studies[6,19] (Extended Data Fig. 5). Cimmeria–Sirenum is the thickest region of the Martian crust that is not directly overlapped by an impact basin, basin ejecta or substantial volcanic deposits. This observation alone (coupled with the unique geochemical and magnetic anomalies of this region) could be viewed as evidence for an ancient origin of the Cimmeria–Sirenum region, without the need for reconstructing the crustal structure of early Mars in any detailed manner.

Do impacts conserve crustal mass?. Impacts can both add material to Mars (from the impactor) and remove material from Mars (in high-speed ejecta). However, for typical impacts, the mass of material excavated and displaced is several orders of magnitude larger than the mass of the impactor, which in turn is generally larger than the mass ejected[35,36]. Impacts also change the density structure of the crust; impacts often generate higher-density, lower-porosity impact melt sheets in the impact basin, while also depositing lower-density, higher-porosity ejecta blankets around the impact basin[37]. Crustal thickness models A and B do not account for density variations in/around impact basins. These density variations probably exist, but are unresolvable in the current geophysical datasets. These variations may slightly alter the crustal reconstruction in/around impact basins.

It is plausible that impact basins do conserve mass, but not in a symmetric fashion. Our method assumes that impacts are axisymmetric, yet all of the features we remove have some axisymmetric structure that is not captured in our reconstruction. For example, Hellas and Borealis are notably elliptical. There is no simple way to relate the ellipticity of the central depression to the asymmetry in the surrounding ejecta blanket and deformation—as these processes do not necessarily share the same symmetry. For example, the South Pole–Aitken basin on the Moon is notably elliptical, yet the associated ejecta deposit is not simply a larger ellipsoid surrounding it[7]. Nonetheless, we considered more complicated fitting schemes that incorporated elliptically symmetric structures, but ultimately opted for the simpler, axisymmetric solution as it reduces the number of fitting parameters and yields qualitatively similar results.

Extended Data Fig. 4 shows the mass balance for each of the features removed in our nominal crustal reconstruction (Fig. 1e,f). Extended Data Fig. 4c shows that our method is able to find mass-conserving solutions for most impact structures, with one specific exception: Utopia Planitia. Utopia Planitia is a large mass deficit (mass deficit > 100 × the mass excess). This mass imbalance is far larger than we anticipate for most impact basins, and is discussed in the next section.

Utopia. Our mass-conservation methodology identified mass-conserving crustal thickness profiles for every impact basin—except Utopia Planitia. Utopia is unique amongst the Martian impact basins in that it is a prominent topographic basin and region of thinned crust, but lacks a significant annulus of excess crustal material around it (Extended Data Fig. 2). There is a small topographic and crustal ring around the basin (~30° away from the centre, most visible in the northwest–northeast), but the mass excess in this ring is >100× smaller than the mass deficit within the basin. It is not clear why Utopia shows such a significant mass imbalance. One possible explanation is that the crustal density in this region is significantly different from that expected in the standard crustal thickness models (models A and B). If the crustal density in the basin or the surrounding annulus were different, it might result in a mass-conserving solution. In fact, our method produces a mass-conserving solution for Utopia when using the spatially varying crustal thickness model of ref. [18] (model C; although for the reasons described above, we are not inclined to use this model for the global crustal structure of Mars). Alternatively, Utopia may be significantly modified by the substantial

sedimentary layer that overlays it. It is conceivable that the deposition and erosion of this material affected the crustal structure in some non-axisymmetric way. Regardless, a detailed study of the Utopia basin is left for future work.

Borealis and the hemispheric dichotomy. In this work, we focused on removing the crustal signature of the four largest, unequivocal impact basins (Hellas, Argyre, Utopia and Isidis). However, some researchers have suggested that the geometry and geophysical structure of the northern lowlands may be the diagnostic signature of one or more giant impact basins[2,3,6,38,39]. The existence of a 'Borealis' impact basin is still debated, so we did not include it in our primary analysis. Nonetheless, we did experiment with adding Borealis into our reconstruction, and we discuss those results here.

Extended Data Fig. 5 shows what happens when we take our nominal model (Fig. 1e,f), and use our mass-conservation technique to remove Borealis. As Borealis is truly global, we had to augment our mass-conservation approach. Rather than exploring a parameter space of fitting/transition zones (as discussed above), we simply calculated the crustal thickness at which the crustal mass excess above that datum equalled the crustal mass deficit beneath it (using Fig. 1e,f as the initial condition; Extended Data Fig. 5). Phrased a different way, we found the solution where the crustal mass deficit in the northern lowlands is roughly equal to the crustal mass excess in the southern highlands. Removing the contribution of impact basins, volcanoes and Borealis reveals an extremely subdued crustal structure for Mars, with no hemispheric dichotomy (Extended Data Fig. 5). Nonetheless, the Cimmeria–Sirenum region remains an anomalous region of enhanced crustal thickness. Thus, regardless of the veracity of the Borealis impact hypothesis, the Cimmeria–Sirenum crustal block is geophysically distinct.

Data availability

All data used in this study are publicly available on the NASA Planetary Data System Geoscience Node (topography, elemental composition; https://pds-geosciences.wustl.edu/), Planetary Plasma Interactions Node (magnetic field; https://pds-ppi.igpp.ucla.edu/index.jsp) or the NASA Goddard Space Flight Center Planetary Geodynamics Data Archive (crustal thickness; https://pgda.gsfc.nasa.gov/). Source data for the map of Mars's crustal thickness without impact basins and volcanoes (Fig. 1e,f), the primary output of this manuscript, are provided with the paper.

Code availability

All analyses in this study were conducted using original MATLAB code, which is described in the Methods. The MATLAB code is available from J.T.K. upon reasonable request (jkeane@caltech.edu).

References

33. Wieczorek, M. A. in *Treatise on Geophysics* 2nd edn, Vol. 10 (ed. Schubert, G.) 153–193 (Oxford Univ. Press, 2015).
34. Melosh, H. J. *Impact Cratering: A Geologic Process* (Oxford Univ. Press, 1989).
35. Holsapple, K. A. & Housen, K. R. A crater and its ejecta: an interpretation of Deep Impact. *Icarus* **187**, 345–356 (2007).
36. Zhu, M.-H., Wünnemann, K. & Potter, R. W. K. Numerical modeling of the ejecta distribution and formation of the Orientale basin on the Moon. *J. Geophys. Res. Planets* **120**, 2118–2134 (2015).
37. Wieczorek, M. A. et al. The crust of the Moon as seen by GRAIL. *Science* **339**, 671–675 (2013).
38. Marinova, M. M., Aharonson, O. & Asphaug, E. Mega-impact formation of the Mars hemispheric dichotomy. *Nature* **453**, 1216–1219 (2008).
39. Nimmo, F., Hart, S. D., Korycansky, D. G. & Agnor, C. B. Implications of an impact origin for the martian hemispheric dichotomy. *Nature* **453**, 1220–1223 (2008).

Acknowledgements

We thank S. Goossens for kindly sharing crustal thickness and density maps[17]. This research was funded by the Programme National de Planétologie of INSU-CNRS. J.T.K. acknowledges support from the Caltech Joint Center for Planetary Astronomy postdoctoral fellowship. I.M. was financially supported by NASA under grant no. 80NSSC17K0724 issued through the NASA Solar System Workings programme. B.L. was financially supported by a project (NEWTON) that has received funding from the European Union's Horizon 2020 research and innovation programme under grant agreement 730041. This research has made use of NASA's Astrophysics Data System.

Author contributions

S.B. first identified the anomalous crustal structure of Cimmeria–Sirenum. S.B. and D.B. developed the hypothesis and its implications, and guided the research effort. J.T.K. created and executed the crustal thickness correction method and created all figures. The manuscript was collectively written by J.T.K., S.B. and D.B. (in order of the importance of the contribution). I.M. performed preliminary calculations of Mars without Tharsis. B.L. provided the Martian magnetic field model. All authors provided input on the manuscript and the broader implications of this work.

Competing interests

The authors declare no competing interests.

Additional information

Extended data is available for this paper at https://doi.org/10.1038/s41561-019-0512-6.

Supplementary information is available for this paper at https://doi.org/10.1038/s41561-019-0512-6.

Correspondence and requests for materials should be addressed to S.B.

Peer review information Primary Handling Editors: Tamara Goldin; Stefan Lachowycz.

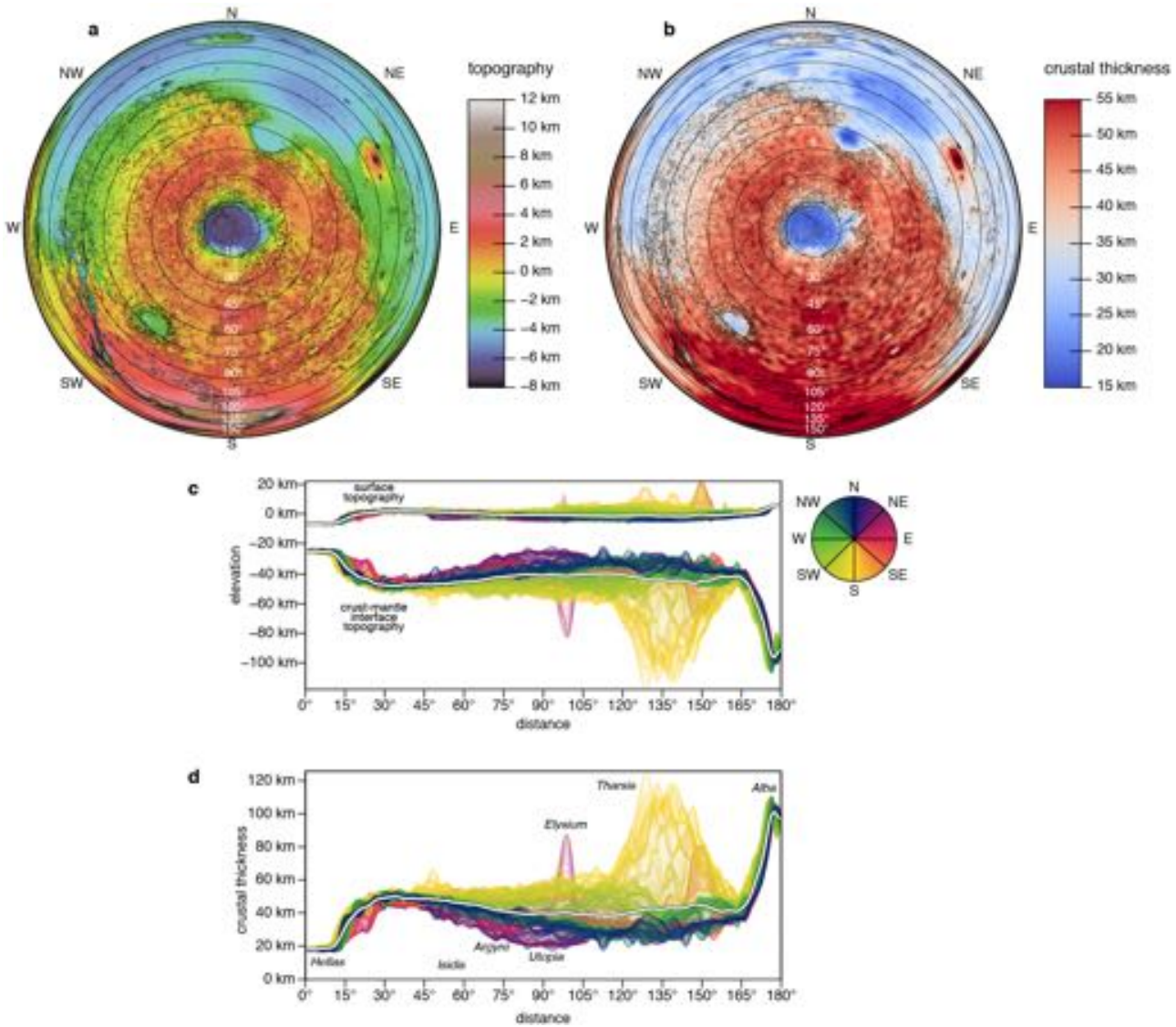

Extended Data Fig. 1 | Topography and crustal structure around Hellas Planitia. a, MOLA topography of Mars (ref. [9]). **b**, crustal thickness of Mars based on crustal model B (ref. [17], Methods). In a–b, the maps are in Lambert azimuthal equal-area projection, centred on Hellas Planitia. Each map covers all of Mars except for a small region antipodal to the map centre. Maps are draped over present-day topography for reference. **c**, radial profiles of surface and mantle topography measured from the centre of Hellas. **d**, radial profiles of crustal thickness. In c–d, each coloured line represented a different radial profile, coloured by the azimuth of that profile. The white lines are the mean of the surface and mantle topography profiles.

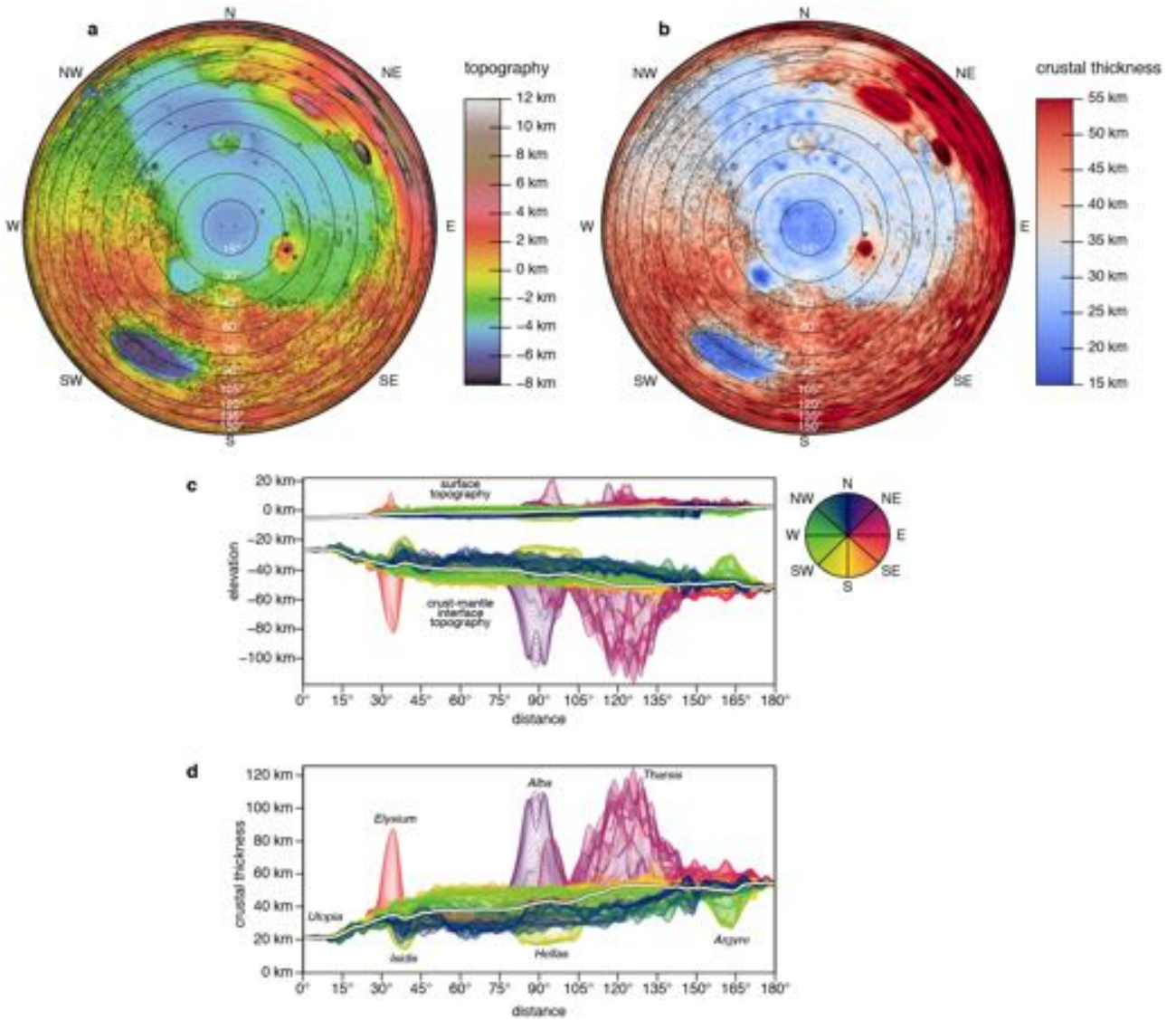

Extended Data Fig. 2 | Topography and crustal structure around Utopia Planitia. a, MOLA topography of Mars (ref. [9]). **b**, crustal thickness of Mars (ref.[17]). In a–b, the maps are in Lambert azimuthal equal-area projection, centred on Utopia Planitia. Each map covers all of Mars except for a small region antipodal to the map centre. Maps are draped over present-day topography for reference. **c**, radial profiles of surface and mantle topography measured from the centre of Utopia. **d**, radial profiles of crustal thickness. In c–d, each coloured line represented a different radial profile, coloured by the azimuth of that profile. The white lines are the mean of the surface and mantle topography profiles.

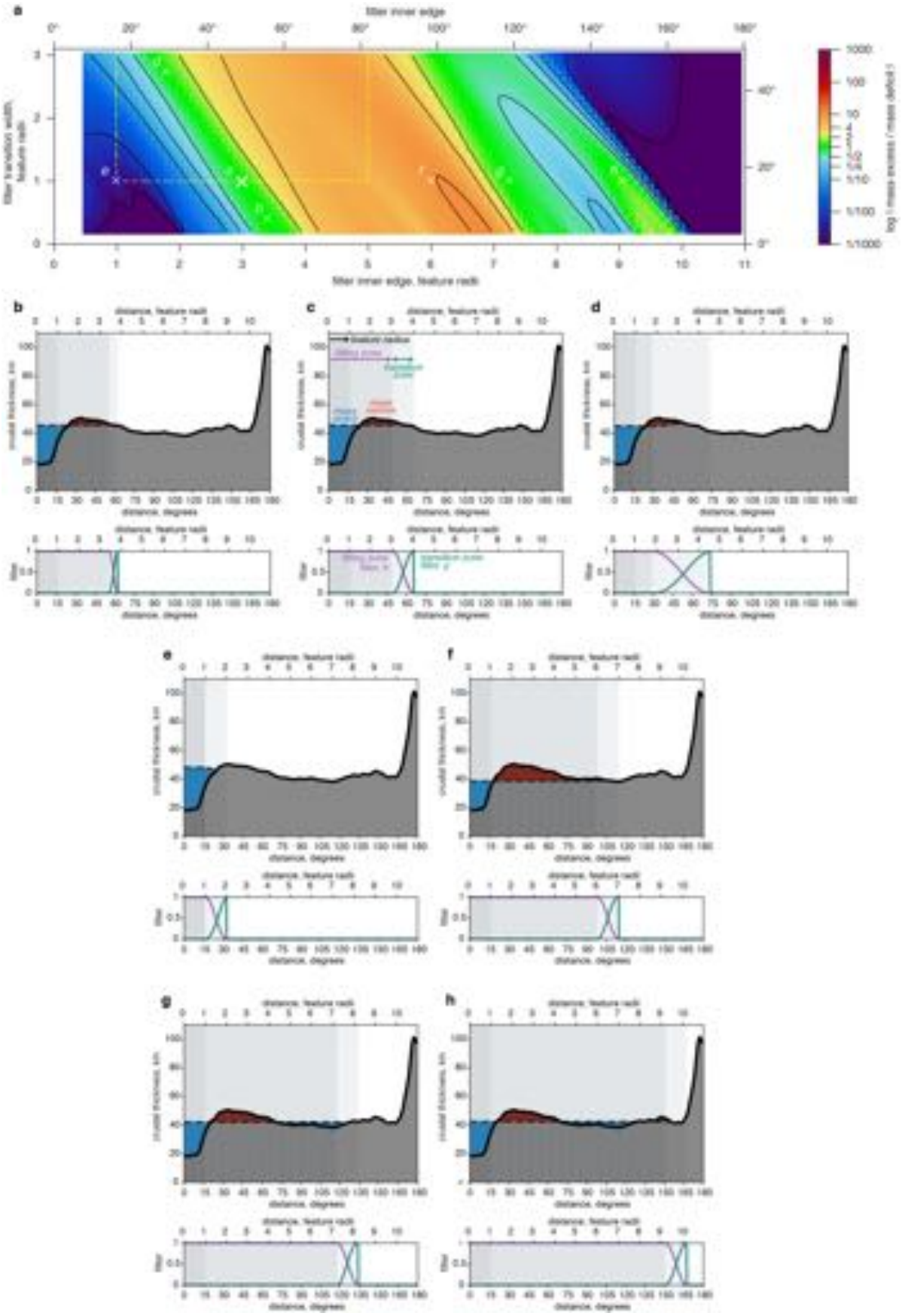

Extended Data Fig. 3 | See next page for caption.

Extended Data Fig. 3 | The parameter space for finding the mass-conserving crustal structure for Hellas Planitia. a, the fitting parameter space. Colour and contours show how well each tested model conserves mass: reds are models dominated by mass excesses, blues are models dominated by mass deficits, and green are models where mass is approximately conserved. Contour levels are indicated by tick marks in the colour bar. The yellow dash-dot region indicates the confining region where we look for the best mass-conserving solutions that are plausibly the result of Hellas. **b–h**, example solutions from the parameter space (marked with an 'x' in panel a). Symbols and lines are the same as in Fig. 2, and are labelled in panel c. In this example model run, panel c is the best-fitting model.

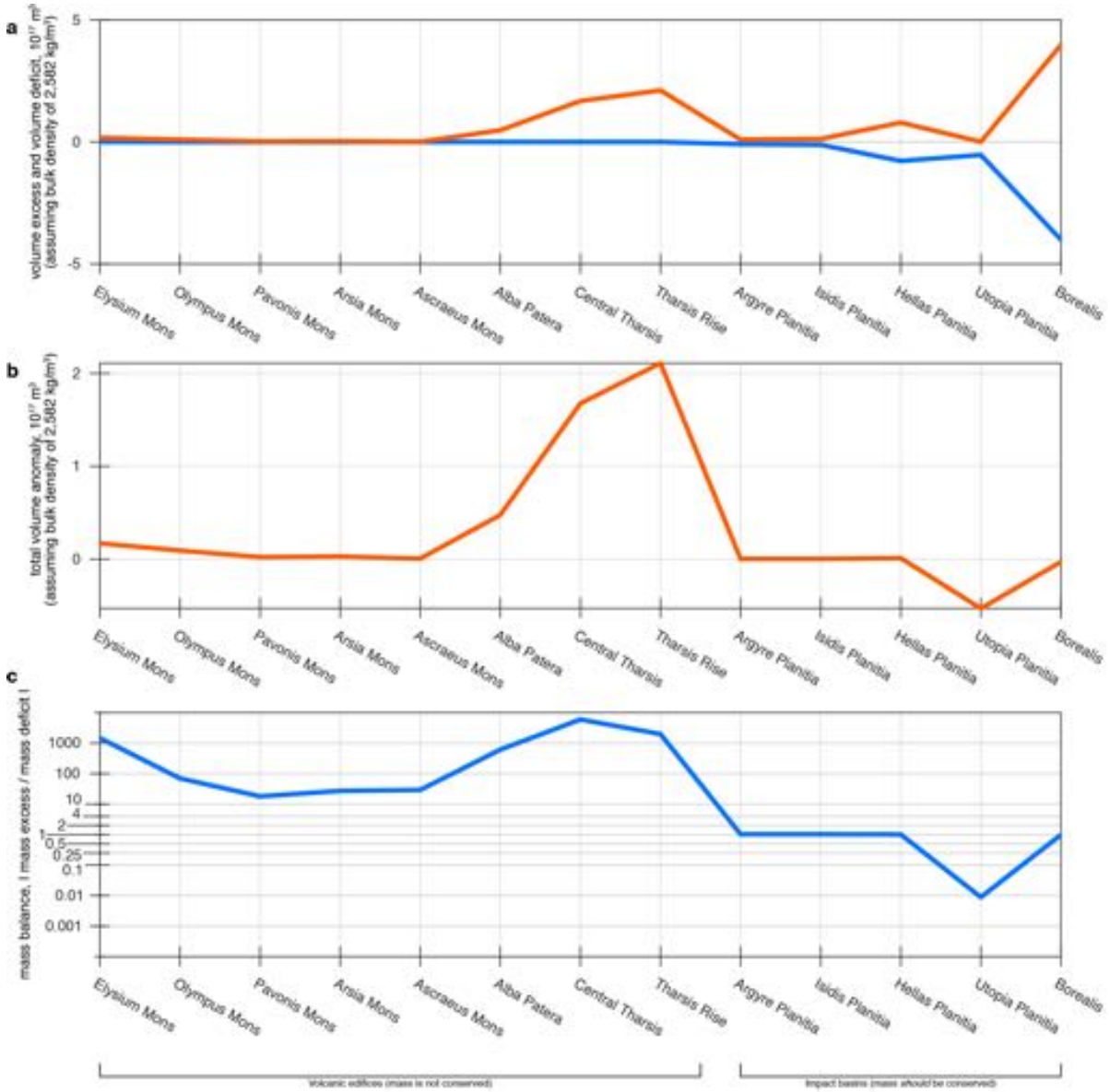

Extended Data Fig. 4 | Mass balance for each feature of interest removed in our crustal reconstruction. a, mass excess (red) and mass deficit (blue) for each feature of interest. **b**, the total mass excess (mass excess + mass deficit) for each feature of interest. Mass-conserving structures have a total mass excess of zero. **c**, the ratio between mass excess and mass deficit. Mass-conserving structures have a ratio of one.

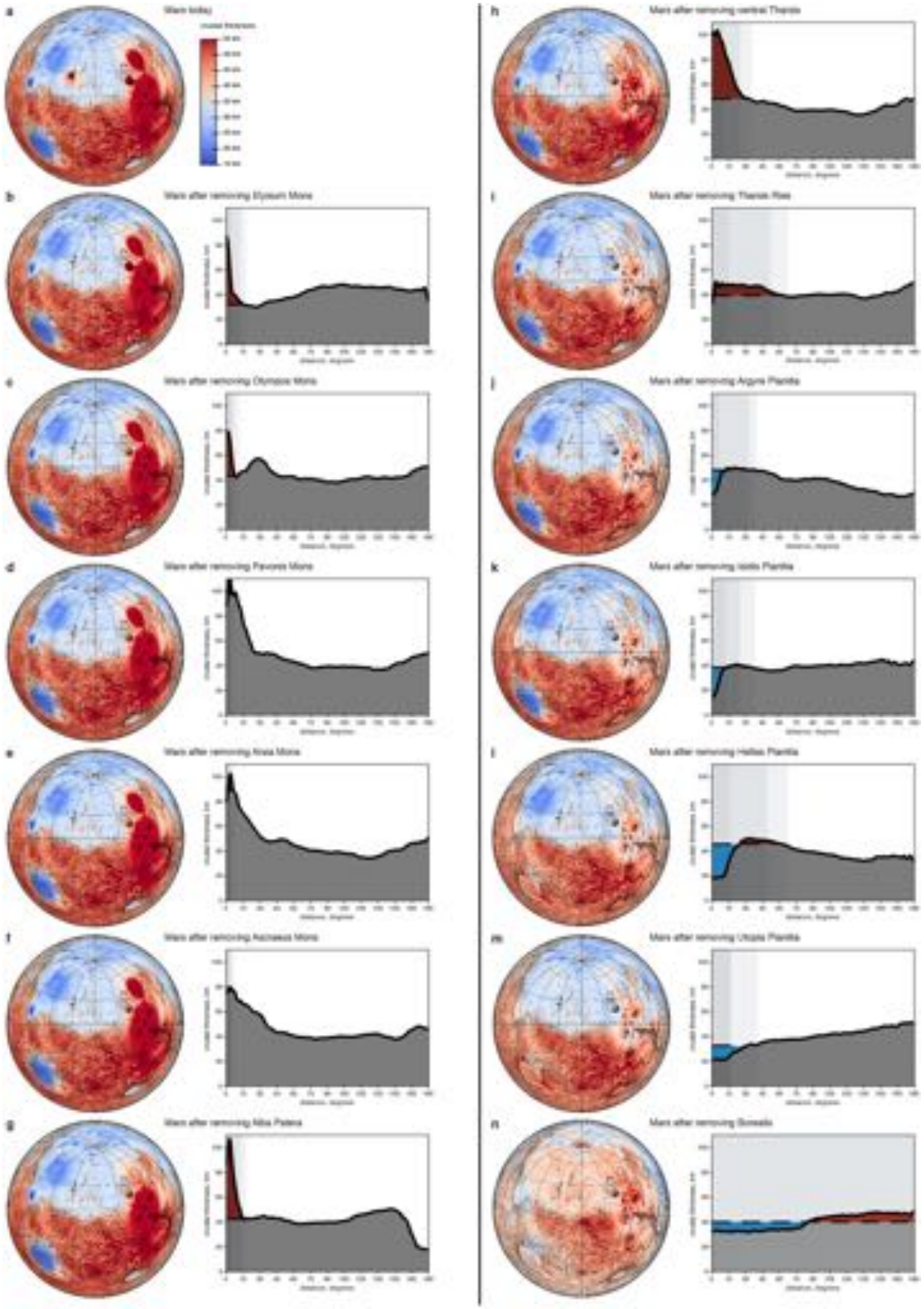

Extended Data Fig. 5 | Crustal thickness map and simplified radial profile after the removal of each feature. a, Mars today. **b**, removing Elysium Mons. **c**, removing Olympus Mons. **d**, removing Pavonis Mons. **e**, removing Arsia Mons. **f**, removing Ascraeus Mons. **g**, removing Alba Patera. **h**, removing central Tharsis. **i**, removing Tharsis rise. **j**, removing Argyre. k, removing Isidis. l, removing Hellas. m, removing Utopia. n, removing Borealis. On simplified radial profiles, the mass excess is in red and the mass deficit in blue.

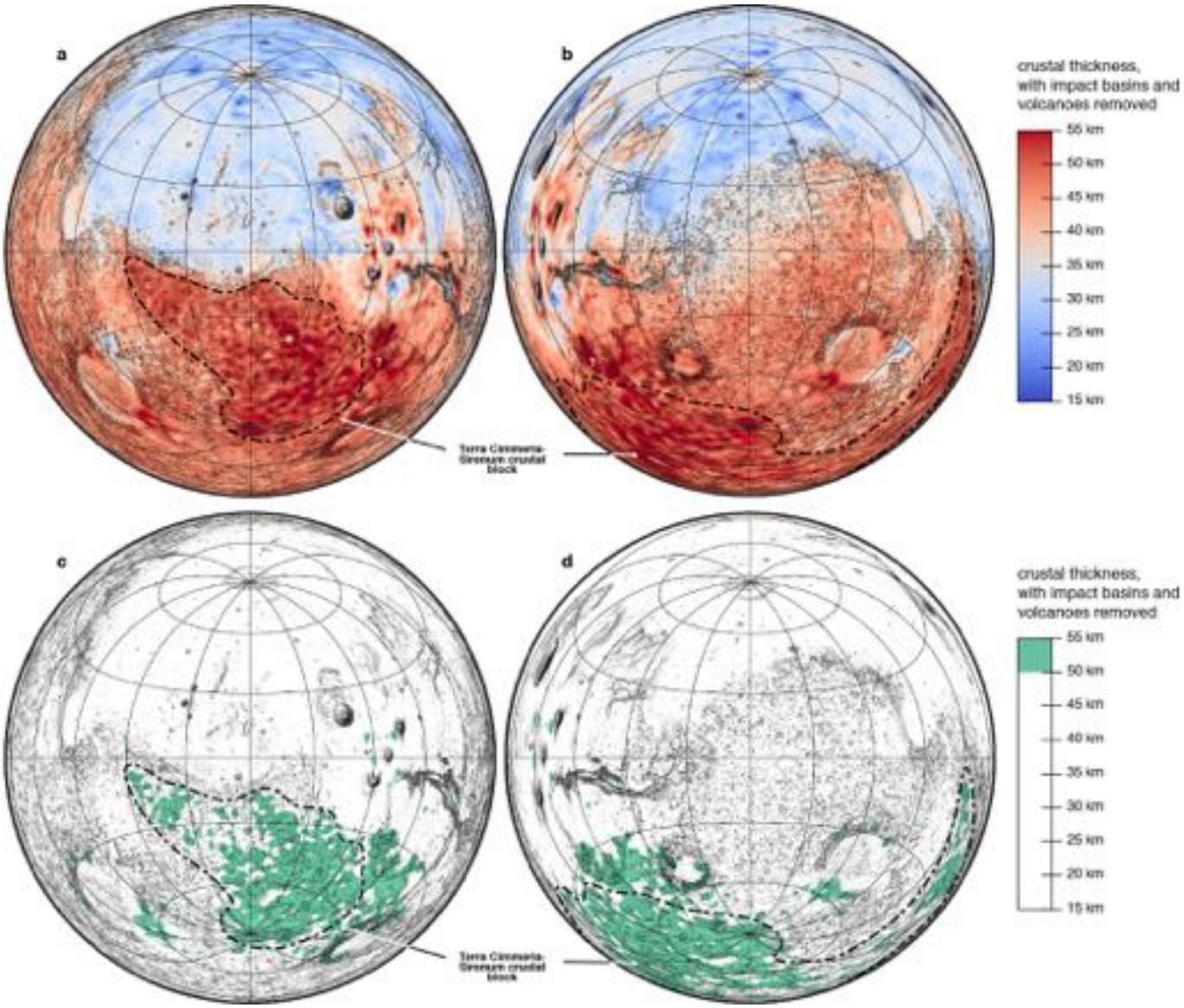

Extended Data Fig. 6 | Boundary of the Cimmeria-Sirenum block with >50 km thick crustal regions indicated in green (c-d). The question mark to the east of the block indicates the unclear boundary between the Thaumasia region and the Cimmeria-Sirenum block due to the possible different origin of Thaumasia[19].

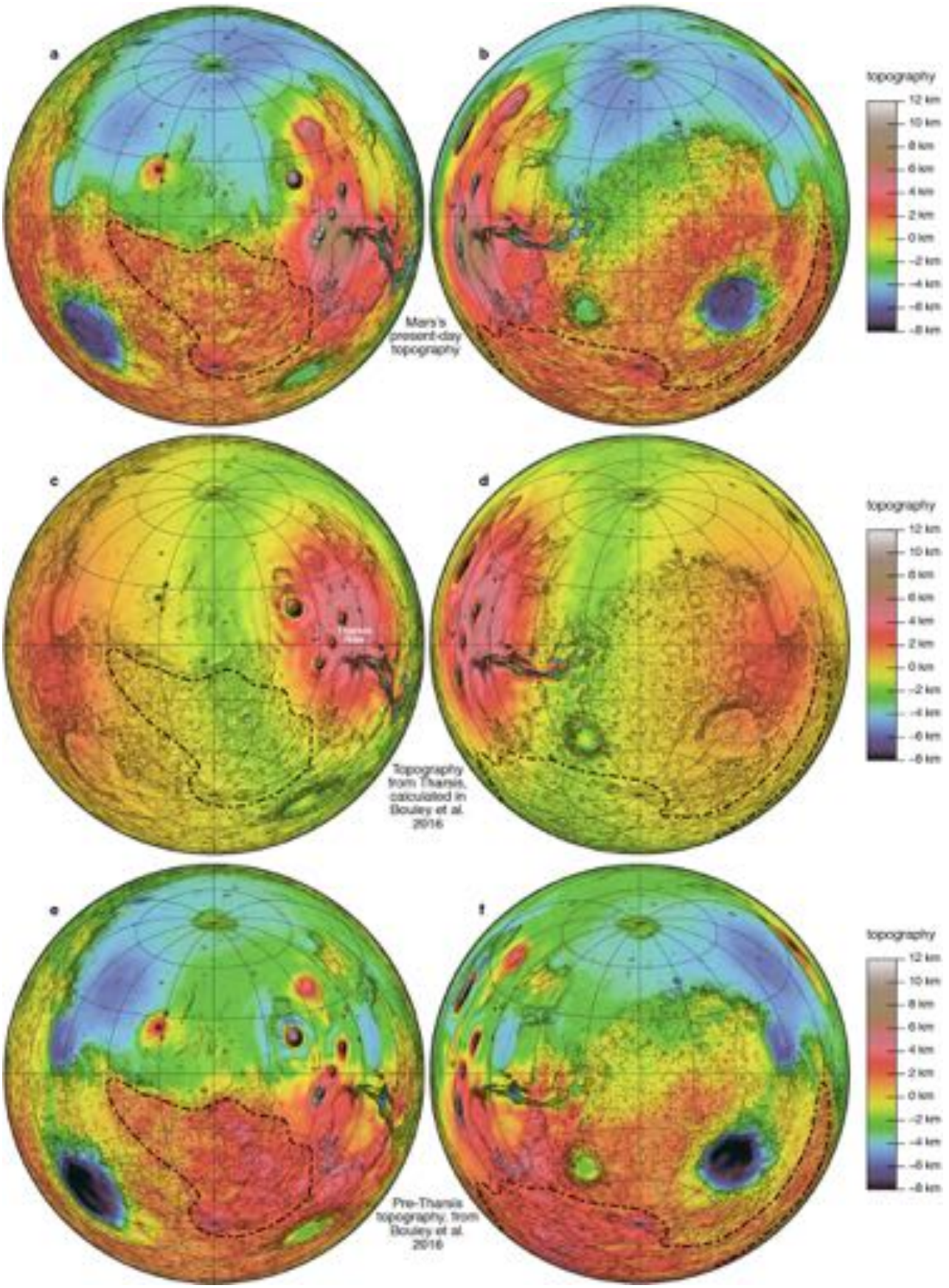

Extended Data Fig. 7 | See next page for caption.

Extended Data Fig. 7 | Topography before Tharsis. a–b, MOLA topography of Mars (ref. [9]), with the Cimmeria–Sirenum region outlined. **c–d**, topographic model of Tharsis, and the rotational deformation arising from TPW due to the formation of Tharsis (ref.[20]). **e–f**, topography of Mars without the effects of Tharsis. Panel e is equal to panel a minus panel c; panel f is equal to panel b minus panel d. The Cimmeria–Sirenum region has anomalously high topography in this corrected map. This early work hinted at the unusual nature of this terrain. Maps are in Lambert azimuthal equal-area projection, centred on 0°E (left column) and 180°E (right column). Each map covers all of Mars except for a small region antipodal to the map centre. Maps are draped over present-day topography for reference. Grid lines are in increments of 30° of latitude and longitude.